SUPPLEMENTAL MATERIAL

Table S1, Figure S1–S2, Video S1

Deep-sea hiatuses track the vigor of Cenozoic ocean bottom currents

Adriana Dutkiewicz & R. Dietmar Müller

Geology, 2022, DOI:10.1130/G49810.1

Correspondence to: adriana.dutkiewicz@sydney.edu.au

Table S1. Details of ODP, DSDP and IODP drill holes used in the analysis of hiatus distributions. Maximum (max) and minimum (min) ages indicate the age range of the age-depth models from the NSB (Neptune Sandbox Berlin) database (https://nsb.mfn-berlin.de; accessed on 17th of February, 2021).

Hole	Long. (°)	Lat. (°)	Water depth (m)	Max age (Ma)	Min age (Ma)
21	-30.598	-28.585	2113	79.3	66.0
62A	141.938	1.870	2602	23.4	0.0
63	147.890	0.836	4486	30.8	0.2
64	158.610	-1.742	2060	39.0	0.0
96	-85.763	23.743	3439	57.3	17.8
125	20.429	34.625	2782	4.9	0.0
132	11.441	40.262	2835	8.6	0.0
137	-27.061	25.926	5361	103.1	93.8
141	-23.999	19.419	4148	9.9	1.2
158	-85.236	6.623	1953	12.9	0.2
167	-176.825	7.068	3176	83.0	64.6
170	177.617	11.800	5792	84.3	71.1
171	-169.460	19.132	2290	90.4	52.9
173	-125.452	39.962	2927	18.3	0.3
178	-147.131	56.956	4218	23.1	0.5
192	164.714	53.010	3014	7.1	0.0
208	161.221	-26.110	1545	69.3	0.0
213	93.896	-10.212	5611	7.0	0.7
216	90.208	1.462	2247	66.3	23.8
217	90.539	8.926	3020	66.4	24.8
233	52.135	14.328	1839	3.1	0.3
236	57.648	-1.677	4487	23.8	0.5
238	70.526	-11.154	2832	24.2	0.1
253	87.366	-24.878	1962	23.0	0.5
258	112.474	-33.795	2793	108.5	83.8
265	109.946	-53.541	3581	9.9	0.1
266	110.112	-56.402	4173	20.3	0.2

267B	104.488	-59.262	4522	14.1	1.6
277	166.191	-52.224	1214	56.4	0.0
278	160.071	-56.557	3675	36.7	0.1
281	147.764	-47.997	1591	23.5	0.0
289	158.512	-0.499	2206	60.9	1.0
296	133.525	29.340	2920	29.6	0.0
305	157.850	32.002	2903	134.5	66.1
317B	-162.263	-11.002	2598	22.9	0.1
327A	-46.784	-50.871	2400	127.4	0.0
338	5.388	67.785	1297	50.0	34.0
354	-44.196	5.899	4052	63.3	0.0
355	-30.601	-15.710	4886	111.3	0.0
356	-41.088	-28.287	3175	92.6	1.3
357	-35.560	-30.004	2086	88.9	1.6
362	10.533	-19.758	1325	23.3	1.8
363	9.047	-19.646	2248	63.6	23.7
366	-19.851	5.678	2853	61.1	21.8
366A	-19.851	5.678	2853	23.4	0.0
369A	-14.999	26.593	1752	40.2	14.4
384	-51.663	40.361	3909	65.8	49.1
386	-64.249	31.187	4782	62.5	29.7
390A	-76.112	30.142	2665	127.6	66.4
398D	-10.718	40.960	3910	67.3	24.8
406	-22.090	55.258	2907	43.4	28.8
407	-30.576	63.939	2472	23.7	1.6
408	-28.912	63.377	1624	23.4	1.3
410	-29.476	45.509	2975	11.0	1.4
433A	170.021	44.777	1862	7.0	2.2
436	145.558	39.933	5240	13.4	0.0
438A	143.232	40.629	1552	14.4	0.2
440B	143.929	39.739	4509	6.4	0.4
445	133.208	25.523	3377	43.2	0.2
448	134.874	16.341	3483	32.4	22.7
458	146.934	17.864	3453	22.9	0.1
459B	147.302	17.863	4121	33.0	0.1
462	165.030	7.238	5181	83.7	2.0
463	174.668	21.350	2525	124.8	64.4
470	-117.519	28.908	3549	14.3	0.0
472	-113.995	23.006	3831	14.0	0.0
493	-98.926	16.381	645	20.5	1.1
495	-91.038	12.496	4140	22.2	0.0
499	-90.948	12.676	6108	17.6	0.0
502A	-79.380	11.490	3052	7.3	0.2
503A	-95.637	4.051	3672	8.1	0.3
511	-46.972	-51.005	2589	123.9	32.6
513A	-24.640	-47.583	4373	33.0	3.4

514	-26.855	-46.046	4318	3.8	0.2
516F	-35.285	-30.277	1313	66.5	23.0
517	-38.041	-30.947	2963	3.7	0.0
519	-11.666	-26.137	3769	9.9	0.0
522	-5.130	-26.114	4441	35.7	0.0
524	3.512	-29.484	4796	68.5	50.2
525A	2.985	-29.071	2467	77.2	0.0
534A	-75.382	28.343	4973	147.3	115.5
538A	-85.171	23.850	2820	53.2	0.0
540	-84.371	23.829	2926	59.7	26.9
545	-9.365	33.664	3142	123.5	94.3
547A	-9.350	33.781	3938	103.5	95.5
548	-12.164	48.916	1251	4.9	0.1
548A	-12.164	48.916	1251	64.7	4.8
549A	-13.098	49.088	4561	36.7	23.1
552A	-23.231	56.043	2301	23.3	0.0
558	-37.344	37.770	3754	33.5	22.9
563	-43.767	33.642	3786	32.9	23.0
572A	-113.842	1.435	3893	6.5	0.0
573	-133.310	0.499	4301	9.2	0.3
574	-133.330	4.209	4561	16.7	0.2
577	157.723	32.442	2675	66.4	0.1
578	151.629	33.926	6010	15.2	0.0
579A	153.836	38.628	35737	4.9	0.0
581	159.796	43.927	5476	12.7	4.7
586B	158.498	-0.497	2208	7.7	0.3
587	161.333	-21.185	1101	4.5	0.0
588	161.227	-26.112	1533	11.1	0.3
588A	161.227	-26.112	1533	16.7	11.5
588C	161.227	-26.112	1533	41.3	16.0
590B	163.358	-31.167	1299	19.3	0.8
591	164.449	-31.584	2131	14.8	0.1
592	165.442	-36.473	1088	34.5	0.1
593	167.674	-40.508	1068	35.0	0.1
594A	174.948	-45.524	1204	17.4	0.0
599	-119.881	-19.452	3654	9.5	0.2
603	-70.028	35.494	4633	12.2	1.5
605	-72.609	38.742	2194	66.2	43.1
606	-35.500	37.339	3007	4.5	0.0
607	-32.957	41.001	3427	6.9	0.0
608	-23.088	42.837	3526	39.2	0.0
609	-24.238	49.878	3884	7.1	0.0
610	-18.887	53.222	2417	19.3	0.0
612	-72.774	38.820	1386	69.0	1.4
643A	1.033	67.715	2769	48.0	0.2
646B	-48.369	58.209	3440	9.8	0.0

647A	-45.262	53.331	3869	54.4	0.0
658A	-18.581	20.749	2264	3.8	0.1
659A	-21.026	18.077	3071	22.8	0.0
662A	-11.739	-1.390	3814	3.9	0.3
663A	-11.879	-1.198	3608	2.8	0.1
664D	-23.228	0.107	3802	9.9	0.1
689B	3.100	-64.517	2080	74.8	0.0
690B	1.205	-65.161	2914	59.3	0.0
693A	-14.574	-70.832	2359	26.0	0.0
699A	-30.677	-51.542	3706	55.4	0.0
700B	-30.278	-51.533	3601	83.9	0.1
702B	-26.369	-50.946	3084	60.8	35.1
703A	7.895	-47.051	1796	40.7	23.4
704B	7.421	-46.880	2532	22.8	0.1
707A	59.017	-7.545	1553	37.5	0.0
707C	59.017	-7.545	1553	66.8	33.5
709C	60.552	-3.915	3047	43.2	0.0
710A	60.980	-4.312	3823	31.2	0.1
711A	61.163	-2.743	4439	45.3	0.0
713A	73.394	-4.193	2920	44.3	40.3
714A	73.787	5.060	2041	26.8	0.0
721B	59.865	16.678	1941	11.1	1.9
722A	59.795	16.622	2023	8.0	0.2
724B	57.787	18.463	591	3.5	0.7
728A	57.826	17.680	1422	9.3	0.0
731A	59.703	16.471	2359	12.1	0.2
736A	71.662	-49.403	629	2.6	0.1
737A	73.032	-50.228	564	10.9	1.7
738B	82.788	-62.709	2253	46.2	21.5
738C	82.788	-62.709	2253	66.1	48.6
744A	80.595	-61.579	2307	36.9	0.9
745B	85.854	-59.595	4083	6.5	0.2
746A	85.868	-59.569	4060	11.1	6.6
747A	76.794	-54.811	1695	65.8	0.0
748B	78.998	-58.441	1288	40.7	0.8
748C	78.998	-58.441	1288	65.9	26.3
749B	76.408	-58.717	1070	41.1	23.0
751A	79.815	-57.726	1634	18.6	0.0
752A	93.578	-30.891	1086	62.6	0.0
757B	88.182	-17.024	1650	53.1	0.0
758A	90.361	5.384	2924	62.3	0.0
761B	115.535	-16.738	2189	61.2	47.3
762B	112.254	-19.887	1360	23.5	0.0
762C	112.254	-19.887	1360	144.3	34.1
763B	112.208	-20.587	1368	113.0	75.9
765C	117.575	-15.976	5721	146.4	10.8

766A	110.454	-19.932	3998	134.6	48.1
786A	141.226	31.875	3058	43.9	23.6
794A	138.231	40.190	2811	5.4	0.6
795A	138.967	43.987	3300	3.8	0.2
797B	134.536	38.616	2862	11.3	0.0
798A	134.800	37.038	903	3.3	0.2
800A	152.323	21.923	5686	119.9	70.1
803D	160.540	2.433	3410	22.4	0.0
806B	159.361	0.319	2521	23.0	0.9
807C	156.625	3.606	2806	77.5	31.5
810C	157.846	32.423	2623	18.5	0.2
815A	149.992	-19.151	466	9.2	0.4
815B	-110.572	2.770	3760	12.6	0.3
823B	146.784	-16.616	1638	16.5	0.3
844C	-90.481	7.921	3415	17.1	0.0
845A	-94.591	9.583	3704	16.5	0.0
846D	-90.818	-3.097	3296	7.3	0.5
847B	-95.320	0.193	3334	7.5	0.2
848B	-110.480	-2.994	3853	9.9	0.3
849B	-110.520	0.183	3839	10.9	0.3
850B	-110.521	1.297	3786	11.7	0.0
852C	-110.076	5.293	3860	10.9	0.0
853B	-109.751	7.211	3716	7.7	0.1
859A	-75.853	-45.896	2741	4.5	0.2
871A	172.344	5.557	1255	23.2	0.0
873B	164.921	11.897	1334	16.6	0.1
881C	161.492	47.102	5531	6.8	0.0
882A	167.600	50.363	3244	5.8	0.0
883B	167.769	51.199	2396	43.5	0.1
883E	167.769	51.199	2396	61.3	11.9
884B	168.337	51.450	3825	19.1	0.0
887C	-148.446	54.365	3631	18.1	0.0
889A	-126.868	48.699	1311	3.2	0.4
902D	-72.773	38.935	808	28.0	1.5
903A	-72.817	38.938	444	13.0	6.1
903C	-72.817	38.938	444	23.4	9.4
904A	-72.768	38.863	1123	46.7	0.1
905A	-72.284	38.614	2698	9.5	2.7
906A	-72.767	38.965	913	13.0	0.2
908A	1.361	78.385	1274	2.7	0.0
911A	8.227	80.474	902	17.6	0.2
913B	-6.947	75.489	3318	49.5	30.3
915A	-39.782	63.471	533	42.0	35.9
918A	-38.639	63.093	1869	4.0	0.0
918D	-38.639	63.093	1869	54.3	3.4
925A	-43.489	4.204	3042	43.3	3.5

927A	-44.481	5.463	3314	16.2	0.0
929A	-43.740	5.976	4358	36.8	0.0
929E	-43.740	5.976	4358	57.1	31.6
959A	-2.735	3.628	2091	25.8	0.0
960C	-2.733	3.584	2035	93.8	0.0
961A	-3.059	3.442	2553	59.2	1.7
967A	32.725	34.068	2553	3.9	0.1
967E	32.725	34.068	2553	93.4	30.2
974B	12.142	40.356	3454	6.5	0.0
975B	4.510	38.896	2416	5.2	0.0
997A	-75.469	31.843	2770	5.6	0.2
997B	-75.469	31.843	2770	6.3	3.6
1049A	-76.112	30.142	2656	122.4	42.0
1050C	-76.235	30.100	2297	104.6	62.2
1051A	-76.358	30.053	1983	63.9	38.3
1052A	-76.627	29.952	1345	41.4	35.2
1052E	-76.627	29.952	1345	103.6	39.9
1053A	-76.524	29.992	1630	39.2	36.6
1067A	-11.596	40.683	5021	58.4	42.3
1068A	-11.612	40.683	5044	69.4	47.1
1069A	-11.777	40.727	5075	76.8	44.0
1088B	13.563	-41.136	2081	9.7	0.0
1088C	13.563	-41.136	2081	13.2	10.4
1089A	9.894	-40.936	4619	2.0	0.0
1090B	8.900	-42.914	3699	42.2	0.1
1091A	5.919	-47.095	4361	3.1	0.2
1092A	7.080	-46.412	1976	14.8	0.0
1093D	5.865	-49.977	3624	4.0	0.4
1094D	5.130	-53.180	2808	1.6	0.3
1095A	-78.487	-66.986	3842	3.0	0.0
1095B	-78.487	-66.986	3842	9.3	2.2
1138A	75.975	-53.552	1141	69.1	0.0
1143A	113.285	9.362	2771	10.5	0.0
1168A	144.413	-42.610	2463	37.1	0.0
1170A	146.050	-47.151	2705	29.7	0.3
1170D	146.050	-47.151	2705	42.8	27.2
1171C	149.112	-48.500	2148	34.7	0.0
1171D	149.112	-48.500	2148	59.0	20.0
1172A	149.928	-43.960	2622	53.5	0.0
1179C	159.963	41.080	5564	17.5	0.0
1207B	162.751	37.791	3101	126.3	0.0
1208A	158.202	36.127	3346	81.8	0.0
1209A	158.506	32.652	2387	69.1	0.0
1210B	158.259	32.224	2574	79.2	0.0
1211B	157.850	32.002	2908	71.0	0.0
1212B	157.712	32.448	2683	101.9	0.0

1213A	157.298	31.577	3883	110.7	0.0
1214A	157.479	31.867	3402	134.2	98.9
1218A	-135.367	8.889	4826	41.2	4.1
1219A	-142.016	7.800	5063	55.6	0.0
1220A	-142.758	10.177	5218	42.0	0.0
1220B	-142.758	10.177	5218	52.9	25.3
1256B	-91.934	6.737	3635	13.5	0.0
1258A	-54.733	9.433	3192	107.6	46.2
1260A	-54.544	9.266	2549	103.1	29.1
1262B	1.577	-27.186	4759	67.2	0.0
1263A	2.779	-28.533	2717	59.4	0.7
1264A	2.846	-28.533	2507	30.0	0.7
1265A	2.639	-28.835	3060	57.7	0.3
1266A	2.344	-28.543	3800	57.9	0.0
1267B	1.711	-28.098	4354	68.4	0.0
1302A	-45.638	50.166	3569	1.1	0.0
1304A	-33.530	53.057	3069	1.8	0.0
1308A	-24.238	49.878	3871	3.3	0.0
1313A	-32.957	41.001	3412	6.3	0.0
1314A	-27.889	56.365	2799	2.8	0.0
1331A	-142.162	12.068	5121	52.5	0.0
1332B	-141.046	11.912	4918	47.7	0.8
1333A	-138.420	10.517	4859	45.0	20.0
1334A	-131.973	8.000	4793	37.9	0.0
1335A	-126.283	5.312	4333	26.1	0.0
1336A	-128.254	7.701	4291	32.0	12.5
1337A	-123.206	3.833	4466	23.4	0.0
1338A	-117.969	2.508	4205	17.7	0.0
1403A	-51.803	39.943	4944	76.8	35.5
1404A	-51.810	40.013	4742	43.2	0.0
1405A	-51.820	40.138	4286	26.6	0.4
1406A	-51.650	40.350	3815	59.6	0.0
1407A	-49.813	41.425	3073	103.0	31.7
1408A	-49.786	41.438	3022	58.2	0.0
1409A	-49.233	41.296	3503	62.0	0.0
1410A	-49.170	41.328	3387	53.1	0.0
1411B	-49.000	41.618	3299	38.0	0.3

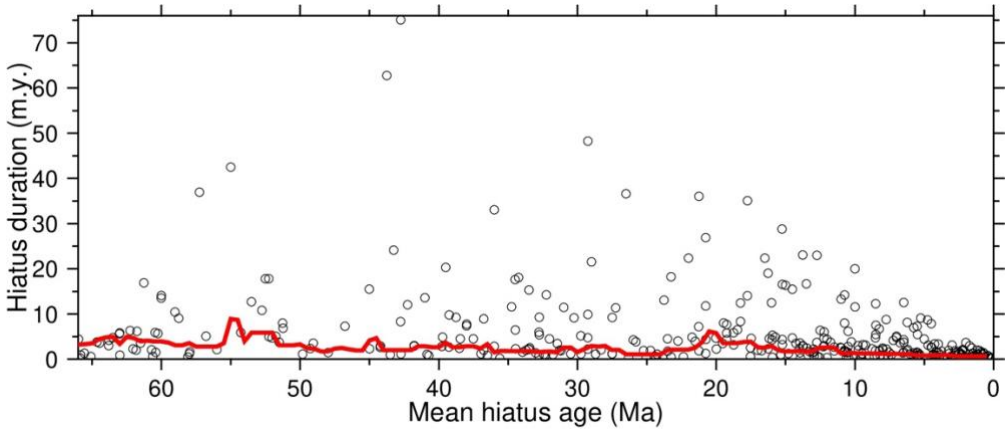

Figure S1. Hiatus duration and mean hiatus age for all hiatuses used in the analysis. Red line shows the mode of hiatus duration computed using a 5 m.y. moving window and a robust maximum likelihood probability filter. The mode is relatively constant for hiatuses aged between 50 Ma and 0 Ma, showing a slight increase prior to 50 Ma.

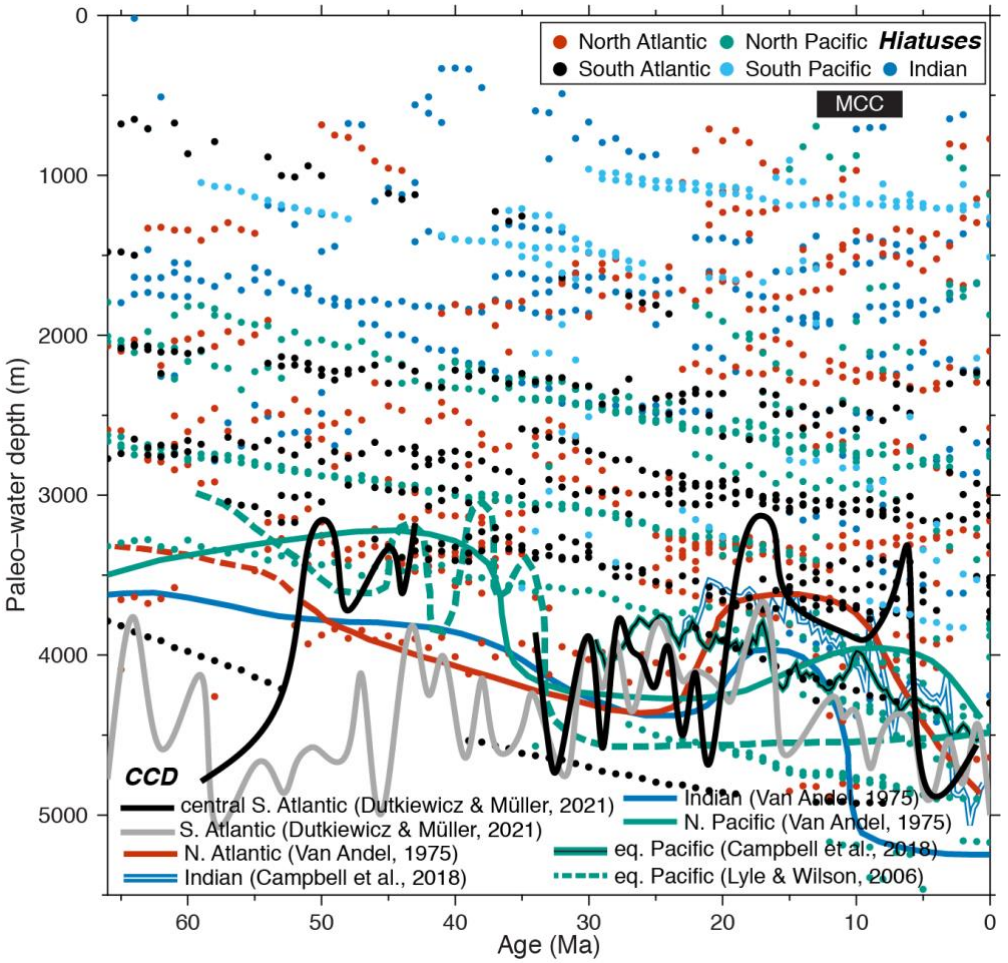

Figure S2. Hiatus paleo-water depths and their ages in 1 m.y. bins for the entire range of paleo-water depths. Miocene carbonate crash (MCC) based on compilation of Torfstein and Steinberg (2020).

Video S1. Distribution of deep-sea hiatuses (pink dots) and non-hiatuses (yellow dots), and their paleo-water depths for the Cenozoic. Orange regions denote contourite drifts based on estimated maximum ages of their formation from the compilation of Thran et al. (2018). Paleobathymetry of preserved seafloor is reconstructed using pyBacktrack (Müller et al., 2018) while paleo-water depths of now subducted ocean floor (smooth regions) are based on Wright et al. (2020). Note that data at present-day are not used in our analysis because core tops are often missing from drilled sections. Black areas indicate continents and grey areas indicate regions where paleobathymetric reconstruction was not possible due to a poor knowledge of lithospheric extension or where continental crust was exposed. Paleobathymetry reconstruction of submerged continental crust depends on knowledge of the rift start and end time as well as the lithospheric stretching factor for a given site, taken from a plate model which includes plate deformation (Müller et al., 2019). These parameters are poorly constrained in some tectonically complex regions (e.g., some Southeast Asian marginal seas), resulting in an exclusion of a small number of points from paleobathymetry analysis. However, this nearly exclusively affects reconstructed conformities, not hiatuses.White lines are mid-ocean ridges, and white lines with teeth are subduction zones. Mollweide projection.

References:

Müller, R. D., Cannon, J., Williams, S., and Dutkiewicz, A., 2018, PyBacktrack: a tool for reconstructing paleobathymetry on oceanic and continental crust: Geochemistry, Geophysics, Geosystems, v. 19, p. 1898–1909, https://doi.org/10.1029/2017GC007313.

Müller, R. D., Zahirovic, S., Williams, S. E., Cannon, J., Seton, M., Bower, D. J., Tetley, M. G., Heine, C., Le Breton, E., and Liu, S., 2019, A global plate model including lithospheric deformation along major rifts and orogens since the Triassic: Tectonics, v. 38, p. 1884-1907, https://doi.org/10.1029/2018TC005462.

Thran, A. C., Dutkiewicz, A., Spence, P., and Müller, R. D., 2018, Controls on the global distribution of contourite drifts: Insights from an eddy-resolving ocean model: Earth and Planetary Science Letters, v. 489, p. 228-240, https://doi.org/10.1016/j.epsl.2018.02.044.

Torfstein, A., and Steinberg, J., 2020, The Oligo–Miocene closure of the Tethys Ocean and evolution of the proto-Mediterranean Sea: Scientific Reports, v. 10, p. 1-10, https://doi.org/10.1038/s41598-020-70652-4.

Wright, N. M., Seton, M., Williams, S. E., Whittaker, J. M., and Müller, R. D., 2020, Sea level fluctuations driven by changes in global ocean basin volume following supercontinent break-up: Earth-Science Reviews, p. 103293, https://doi.org/10.1016/j.earscirev.2020.103293.